Chalmers Publication Library

On Coordinated Control of OLTC and Reactive Power Compensation for Voltage Regulation in Distribution Systems With Wind Power

(article starts on next page)

On coordinated control of OLTC and reactive power compensation for voltage regulation in distribution systems with wind power

S.N. Salih, P. Chen, *member, IEEE*

Abstract—Active management strategies such as coordinated on load tap changer (OLTC) voltage control and reactive power compensation (RPC) are frequently suggested for voltage regulation in a distribution system with a high level of distributed generation (DG). This paper proposes a control and coordination algorithm for these two active management strategies. Voltage control through OLTC is achieved by using state estimation (SE) to determine the voltage in the network. To lower the implementation cost of the proposed control strategy, pseudo-measurements are used together with real-time measurement data in the SE. Moreover, the deadband of the automatic voltage control (AVC) relay is relaxed so that the AVC relay acts on the network's maximum or minimum voltage obtained through the SE. This is found to be simpler to realize than adjusting the set point of the AVC relay. Voltage control through RPC is actualized by using integral controllers implemented locally at the wind turbine site. Furthermore, RPC from the local wind turbine is also used to mitigate an overvoltage at a remote bus on the same feeder when the remote wind turbine reaches its regulation limit. The applicability of the proposed voltage regulation algorithm is successfully demonstrated using a case study system.

Index Terms—Wind power, Voltage control, active management schemes, distribution system

Nomenclature

AVC	Automatic voltage control
DG	Distributed generation
DSSE	Distribution system state estimation
MPP	Maximum power point
OLTC	On load tap changer
RPC	Reactive power compensation
SE	State estimation

Sets & Indices

i, j	Bus indexes of the network
l	Measurement points in the network

Variables

$E_{th,r}$	The real part of the Thevenin voltage seen from the wind turbine terminal [p.u.]
E_{th}	The Thevenin voltage seen from the wind turbine terminal [p.u.]
$f_l(\mathbf{x})$	The measurement function that relate the state vector with measurement l
I_d	The d-axis component of the current vector [p.u.]

I_d^{ref}	The reference for the d-axis component of the current vector [p.u.]
P_i	The net active power injected at bus i [p.u.]
P_w	The active power output of the wind turbine [p.u.]
P_w^{ref}	The active power reference to the wind turbine controller [p.u.]
Q_{measured}	Measured reactive power output of the wind turbine [p.u.]
Q_i	The net reactive power injected at bus i [p.u.]
Q_w	The reactive power output of the wind turbine [p.u.]
Q_w^{ref}	The reactive power reference to the wind turbine controller [p.u.]
R_{th}	The calculated Thevenin resistance seen from the wind turbine terminal [p.u.]
V_w^0	Assumed voltage magnitude at the wind turbine terminal [p.u.]
V_w^{ac}	Actual voltage magnitude at the wind turbine terminal [p.u.]
V_{local}	voltage level at the terminal of the local wind turbine [p.u.]
V_{measured}	Measured voltage at the terminal of the wind turbine [p.u.]
V_{ref}	The voltage reference to the reactive power PI controller [p.u.]
V_{remote}	voltage level at the terminal of the remote wind turbine [p.u.]
V_{set}	The voltage set point of the AVC relay [p.u.]
v_d	The d-axis component of the voltage vector [p.u.]
V_i	Voltage magnitude at node i [p.u.]
V_{lb}	The magnitude of the lower bound voltage $1 - \Delta V$, e.g. 0.95, [p.u.]
V_{ub}	The magnitude of the upper bound voltage $1 + \Delta V$, e.g. 1.05, [p.u.]
V_w	Voltage magnitude at the wind turbine terminal [p.u.]
$\hat{V}_i$	Voltage magnitude estimate at Bus i [p.u.]
$\hat{V}_{\text{min/max}}^k$	The voltage signal estimate sent to the AVC relay by the voltage level analyzer [p.u.]
$\hat{\mathbf{V}}^k$	The voltage magnitude estimate vector of the network at time k [p.u.]
$\mathbf{x}$	The state vector
X_{th}	The calculated Thevenin reactance seen from the wind turbine terminal [p.u.]
X_{th}^{ac}	The actual value of the Thevenin reactance seen from the wind turbine terminal [p.u.]
$Y_{i,j}$	Magnitude of the $(i, j)^{th}$ element of the bus admittance

	matrix [p.u.]
$\mathbf{z}$	The measurement data vector
z_l	Measurement at point l
ΔV	The allowed voltage variation in the network around the nominal voltage level, e.g. 0.05, [p.u.]
ε_Q	A small positive value,e.g. 0.025, [p.u.]
ω	The rotational speed of the wind turbine [p.u.]
δ_i	Voltage angle at node i [rad]
$\varepsilon_{v,r}$	The additional change in voltage above the upper bound that triggers the RPC of other wind turbine, e.g. 0.001, [p.u.]
$\boldsymbol{\sigma}_v^k$	Vector of the standard deviation of voltage estimates at time k [p.u.]
σ_l	Standard deviation of the lth measurement
$\theta_{i,j}$	Angle of the $(i,j)^{th}$ element of the bus admittance matrix [rad]

I. INTRODUCTION

THE integration of wind power and other distributed generation (DG) to weak rural distribution system is mainly limited due to voltage rise problems. Though the wind power hosting capacity of these distribution networks can be increased using traditional solutions such as grid reinforcement, these solutions are not cost effective. Consequently, active management schemes such as reactive power compensation (RPC) and coordinated OLTC voltage control have been widely studied as a cost effective alternative of increasing the hosting capacity of these networks [1]–[4]. A large number of research work have also been devoted to the investigation of the control and implementation of these active management schemes [5]–[21]. Though the ultimate aim of either RPC or coordinated OLTC voltage control is to maintain the voltage within a given deadband, e.g. ±5%, various research works have proposed different control algorithms to achieve the same. Moreover, some of the works only investigate the use of OLTC for voltage regulation [5]–[10], and some others only investigate the control of the terminal voltage of a wind turbine using RPC [11]–[16] while others have proposed algorithms for the control and coordination of both OLTC and RPC for regulating the distribution system voltage [17]–[21].

When it comes to the control algorithms of OLTC for voltage regulation, a number of papers [5]–[8] have proposed a solution in which a number of measurements are obtained from critical locations throughout the network and the voltage set point is changed according to this information. However the identification of the critical points is not an easy task. Others have assumed the availability of voltage measurements from every node [17], [18]. But this is rarely the case in existing rural distribution system. State estimation (SE) based on real-time measurement along with pseudo-measurement is also proposed to determine the voltage level of the network and this information is used to control the target voltage of automatic voltage control (AVC) relays of the substation transformer [9], [19]. In [20], load estimation based on customer class curves together with measurement data at the substation and from remote DG are used to determine the maximum and minimum voltage in the network. Then the appropriate control decision

is taken to limit the voltage in the system within the allowed operating range. Reference [10] proposes to make separate local measurements on feeders with load only and on feeders that contains generation. Based on these measurement data and previous knowledge of load sharing between the different feeders, the power output from the DG is estimated and used to determine the voltage setting required at the substation to mitigate voltage rise at DG terminal. On the other hand, knowing the load in the feeder, the traditional line drop compensation approach is used to determine the voltage setting required to mitigate undervoltage in the system. By combining these two strategies the voltage setting that mitigates undervoltage and overvoltage in the system is determined.

In the case of RPC, References [17], [19] have proposed the use of PI controller where the difference between the voltage set point and the actual voltage level is passed through a deadband to make sure the PI controller works only when the voltage is above the maximum or below the minimum voltage level. In [11], the PI controller is used as well, however, the authors have used a method based on power factor tracking rather than deadband to make sure the PI controller works only when the voltage is above the maximum voltage level. An alternative control approach based on fuzzy logic is also proposed in the same reference. These control approaches ensure that RPC does not unnecessarily increase the power losses in the network. In [12], the aim is to eliminate the voltage rise introduced due to active power injection from the wind turbine. Though this approach keeps the voltage at various points of the system at the same level as before wind power introduction, it increases the power losses in the system. In [13], fuzzy logic based location adaptive droop method is proposed to coordinate RPC from multiple DG for voltage rise mitigation. In [14], RPC using droop control function is proposed to mitigate voltage rise in multiple PV installations in distribution systems. The change in the power losses of the system is also given due consideration. The droop function works based on the amount of active power generation to ensure that the PV are not penalized based on their location, which would happen if the droop function works based on the voltage level at the PV terminal. Moreover, local voltage measurements are used to ensure the proper operation of the droop based compensator. In [15], [16], [20] the required change in reactive or active power to mitigate the voltage rise problem is calculated using sensitivity analysis. In [18] state estimation is used for the same purpose.

Moreover, for the coordination of voltage control through OLTC and RPC, References [17]–[19] have proposed a centralized controller and in [20] the controller at each component (i.e. OLTC or DG) acts as an agent which carries out its control action based on the system state and information it gets from other agents. In [21] the OLTC and the DG in a given feeder are given voltage regulation zones. The OLTC is operated with line drop compensation (LDC) within its allotted working zone while the amount of reactive power required for compensation is determined using a proportional controller which works in a similar fashion as a tap changer with a time delay.

This paper proposes a new control strategy for the voltage rise mitigation by using RPC from wind turbines and OLTC

of the substation transformer. The contributions of the paper include: 1) a strategy that changes the voltage deadband instead of the voltage set point of the AVC relay of the tap changing transformer, 2) coordination of reactive power from multiple wind turbines for voltage regulation, and 3) the coordination of voltage regulation from OLTC and RPC using a higher voltage deadband in the case of OLTC than of RPC.

II. THE CONTROL OF OLTC

In a distribution system where wind turbines are installed, the buses in the network where the lowest or the highest voltage occur depends on the level of load and wind power in the system, i.e. it can not be known with certainty beforehand. Thus the traditional control principles of OLTC can not provide satisfactory voltage regulation in such a network. In principle acquiring the voltage measurements from electricity meters at the consumers end and wind turbines, as assumed in [17], [18], would be ideal, but renders itself to be very expensive when it is not already in place in the system. Even in the presence of smart meters which can provide load and voltage data from every customer nodes (as in Malta, Finland, Italy, Sweden [22]), these data are not available in the frequency that is required for voltage control. The highest data refresh rate currently available is 10 minutes in Italy [22], while for voltage control one need to have a data refresh rate in seconds. Thus, one needs to find an alternative approach which provides an acceptable level of voltage regulation quality without being too expensive. One of the aims of this paper is to show the applicability of using few real-time measurement together with pseudo-measurement to determine the voltage level in the network using SE and provide acceptable level of voltage regulation quality.

A. The state estimation algorithm

There are numerous published works that deal with SE in distribution systems [9], [23]–[27]. The basic principle of SE in these works is similar: minimize the weighted error (based on measurement accuracy) between measured values and calculated values. The calculated values are obtained from measurement functions which are built for each measurement type by using the state vectors. That is,

$$\min_{\mathbf{x}} J(\mathbf{x}) = \sum_{l=1}^{n} \frac{[z_l - f_l(\mathbf{x})]^2}{\sigma_l^2} \tag{1}$$

and the state vectors are iteratively calculated using:

$$\mathbf{x}^{k+1} = \mathbf{x}^k + \left(H^\top(\mathbf{x}^k)W^{-1}H(\mathbf{x}^k)\right)^{-1} H^\top(\mathbf{x}^k)W^{-1}[\mathbf{z} - f(\mathbf{x}^k)] \tag{2}$$

where H is the Jacobian of $f(x)$

$$H(\mathbf{x}^k) = \left[\frac{\partial f(\mathbf{x})}{\partial \mathbf{x}}\right]_{\mathbf{x}=\mathbf{x}^k} \tag{3}$$

and W is the diagonal matrix of measurement covariance:

$$W = \begin{bmatrix} \sigma_1^2 & & \\ & \sigma_2^2 & \\ & & \ddots \end{bmatrix} \tag{4}$$

The difference between the various SE algorithms lies in the choice of the state vector and, hence, on how the equivalent measurement functions are set up and the Jacobian is calculated. In [9], [25], [26], the voltage magnitude and angle is used as state vector while in [23], [24] the author propose to use branch current as state vector. In this paper the node-voltage-based SE is used.

In node-voltage-based SE algorithm one proceeds by developing measurement functions that relate voltage angle and magnitude with measurement data available at each point. Thus, for example, if the measurements available are active and reactive power injection at buses, the measurement function can be given as in (5). Similar equations can be developed when the available measurements are branch currents or power flows [4].

$$\begin{aligned} P_i &= \sum_j Y_{i,j}V_iV_j\cos(\theta_{i,j}+\delta_j-\delta_i) \\ Q_i &= -\sum_j Y_{i,j}V_iV_j\sin(\theta_{i,j}+\delta_j-\delta_i) \end{aligned} \tag{5}$$

The next step is to develop the Jacobian of the measurement function using (3) and the measurement covariance as given in (4). The iterative step of the algorithm starts by setting all bus voltage magnitudes equal to 1 p.u., except in places where voltage magnitude measurements are available, and bus voltage angles to zero. With these initial values of the states one can calculate the initial estimate of the Jacobian matrix $H(\mathbf{x}^0)$ and the measurement functions $f_l(\mathbf{x}^0)$. Then using (2) one can calculate the next estimate of the state vector $\mathbf{x}^1$. The iterative cycle repeats until the objective function $J(\mathbf{x})$ is below a given threshold or the change in the magnitude of the state vector $\Delta\mathbf{x}$ is below a certain small positive value. Once the final estimate of the state vector $\mathbf{x}$ is determined, one can use (6) to calculate the covariance C_x of the state vector $\mathbf{x}$ where the diagonal of the matrix represents the variances of the estimated state variables [26].

$$C_x = (H^\top W^{-1}H)^{-1} \tag{6}$$

Unlike the case of SE in transmission system, SE in distribution system, as presented in this paper, lacks measurement redundancy which makes bad data detection impractical. Therefore, to validate the results of the state estimation, the DSO can use an online voltage measurement data at one or more buses (as required) with lower sampling time (or smart meter data whenever available).

B. The control algorithm

As shown in the block diagram of Fig. 1, the DSSE block estimates the voltage level $\hat{\mathbf{V}}^k$ and the standard deviation $\boldsymbol{\sigma}_v^k$ of the estimates at various buses of the distribution network. Then, based on the voltage estimate from the DSSE block, the voltage level analyzer determines the voltage input to the AVC relay. To ensure an overvoltage or undervoltage is mitigated most (99.7%) of the time, the uncertainty in the estimates is included as $\pm 3\boldsymbol{\sigma}_v^k$. Thus, the output signal of the voltage level analyzer block is determined based on the following logic:
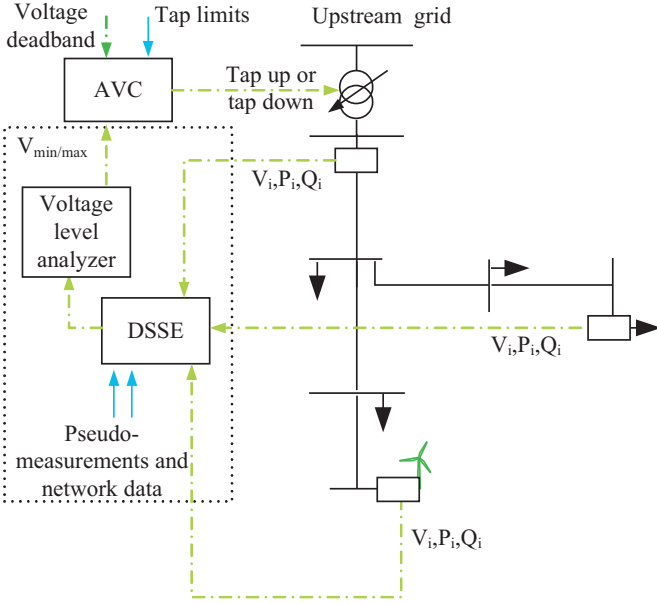
Fig. 1: Block diagram of the proposed OLTC voltage regulation

↪ If $\max(\hat{\mathbf{V}}^k + 3\boldsymbol{\sigma}_v^k - V_{\text{set}}) \leq \Delta V$ p.u. AND $\min(\hat{\mathbf{V}}^k - 3\boldsymbol{\sigma}_v^k - V_{\text{set}}) \geq -\Delta V$ p.u., $\hat{V}_{\text{min/max}}^k = V_{\text{set}}$

↪ Else if $\max(\hat{\mathbf{V}}^k + 3\boldsymbol{\sigma}_v^k - V_{\text{set}}) \geq \Delta V$ AND $\min(\hat{\mathbf{V}}^k - 3\boldsymbol{\sigma}_v^k - V_{\text{set}}) \leq -\Delta V$, $\hat{V}_{\text{min/max}}^k = \hat{V}_{\text{min/max}}^{k-1}$ and Set INFEASIBLE STATE alarm on.

↪ Else if $\max(\hat{\mathbf{V}}^k + 3\boldsymbol{\sigma}_v^k - V_{\text{set}}) \geq \Delta V$, $\hat{V}_{\text{min/max}}^k = \max(\hat{\mathbf{V}}^k + 3\boldsymbol{\sigma}_v^k)$

↪ Else if $\min(\hat{\mathbf{V}}^k - 3\boldsymbol{\sigma}_v^k - V_{\text{set}}) \leq -\Delta V$, $\hat{V}_{\text{min/max}}^k = \min(\hat{\mathbf{V}}^k - 3\boldsymbol{\sigma}_v^k)$

As shown in the block diagram, we propose to change the voltage deadband instead of voltage set point of the AVC relay. One can keep the voltage set point at the nominal value. Under normal operation, the voltage deadband is changed to $\pm$ 5% and the AVC relay sends the Tap-up or Tap-down signal to the OLTC when the voltage obtained from the voltage level analyzer block is outside the given deadband for a given time delay. The AVC relay would also check for the tap limits as it would conventionally do [21].

Due to the lack of measurement redundancy, as mentioned above, if there are measurement errors or a communication failure, the SE may face convergence problems or provide poor confidence on the voltage estimates. If this situation persists for the time delay of the AVC relay, the deadband can be changed to the default value. The voltage set point can be changed to the voltage level at the secondary side of the transformer at the moment of communication failure or convergence problem. The voltage input to the AVC relay would be the voltage level at the secondary side of the transformer. Then, the tap changer would operate as it would traditionally until the problem is resolved.

The OLTC control approach, as presented above, is simpler compared to changing the voltage set point proposed in [5], [7], [9], [17] as the calculation of the voltage set point is not straight forward. In [7] fuzzy logic is used to calculate the

reference voltage while References [5] and [9] have proposed to increase or decrease the voltage set point by a magnitude equal to the voltage deadband. In [17] PI controller is used for the calculation of the voltage set point. However in the proposed approach the AVC relay automatically detects an out of range voltage and sends a Tap-up or Tap-down signal to the tap changer.

III. VOLTAGE REGULATION WITH REACTIVE POWER COMPENSATION

A. The control algorithm

The basic idea of RPC from wind turbines is to consume reactive power when the voltage at the wind turbine terminal is above the allowed level and to inject reactive power whenever the voltage is below the acceptable minimum level. Furthermore, the amount of reactive power consumed or produced should be such that it is just enough to get the voltage back within the allowed deadband.

Not all wind turbine types have this capability of reactive power regulation. Therefore, voltage regulation through RPC mainly deals with Type C, i.e. double fed induction generator (DFIG), and Type D, i.e. full power converter, wind turbines [28]. In the case of Type C wind turbines, although reactive power injection can also be obtained from the grid-side converter, the rotor-side converter is the preferred option for reactive power regulation. The main reason for this is a reactive injection through the rotor circuit is effectively amplified by a factor of 1/slip [29]. In the case of Type D wind turbines, it is the grid-side converter that is used for reactive power regulation [29].

Assuming the cross-coupling and the feed forward terms are properly implemented, the reactive power control loop of the wind turbine can be reduced to the one shown in Fig. 2 in both Type C [30], [31] and Type D wind turbines [32], [33], i.e. a cascade of current control and reactive power control loops. For voltage control through RPC, the reactive power reference to the wind turbine internal controller can be provided as in Fig. 3.
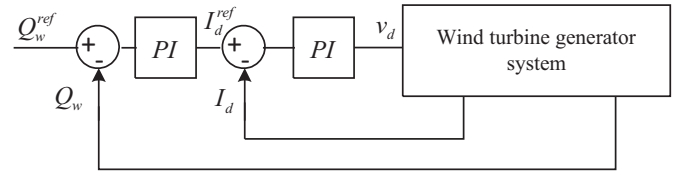

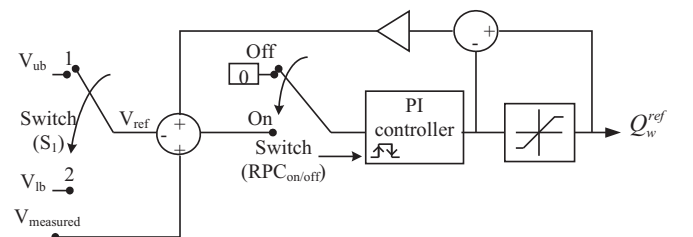Fig. 2: reactive power control in a wind turbine

Fig. 3: Block diagram of a voltage controller

In the block diagram of Fig. 3 there are two switches which are controlled using two separate switching logic. Switch S_1 is set to V_{ub} if the measured voltage is above 1 p.u. otherwise it is set to V_{lb}. In the case of Switch $RPC_{on/off}$ the switching logic is provided in the block diagram of Fig. 4. Whenever $V_{measured}$ is greater than or less than 1 pu by an amount ΔV, the switch $RPC_{on/off}$ is turned on and the RPC is engaged. Once engaged, it will only be turned off, for example, in the case of an overvoltage when $Q_{measured}$ is greater than ε_Q. Here one should note that reactive power is consumed to mitigate an overvoltage. Based on the sign convention adopted here, $Q_{measured}$ is negative for consumption. Thus, the PI controller is turned off when the control algorithm senses that reactive power is being generated rather than being consumed to keep the voltage at V_{ub}. This will avoid the unnecessary use of reactive power to keep the voltage at high values which, on the other hand, may increase the power losses in the system. Here one needs to notice that Switch $RPC_{on/off}$ is also used to reset the PI controller at both rising and falling edge of the switching.
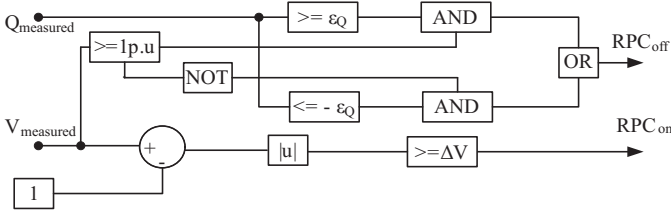

Fig. 4: Block diagram of the switching logic for Switch S_2 in Fig. 3

Note that in Fig.3, it is also possible to provide a direct I_d^{ref} from the voltage controller to the d-axis current controller in Fig. 2 without the need for reactive power controller [29]. But, this paper will only focus on the idea presented in Fig. 3.

The control logic so far enables a wind turbine to regulate the voltage level at its terminal by using RPC with minimum increase in the power losses of the distribution system. One can further use the reactive power capability of a local wind turbine at a given site to mitigate voltage rises at the terminal of a remote wind turbine in the same feeder. This can be valuable if the wind turbine at the remote site has limited or no RPC capability. To carry out the task, the local wind turbine requires the measured voltage at the terminal of the remote wind turbine. To efficiently coordinate RPC from local as well as remote wind turbines, the voltage controller of a wind turbine has two reference voltages: one for the local bus and another for remote buses. Thus, for example, in the case of overvoltage, a wind turbine regulates the voltage at its terminal to be $\leq 1 + \Delta V$ and if the voltage happens to be $\geq 1 + \Delta V$, which shows that the local wind turbine is incapable to regulate the voltage at its terminal, then the other wind turbine in the network will try to limit the voltage at $\leq 1 + \Delta V + \varepsilon_{v,r}$. Here, two inputs to the PI controller is changed, one is the measured voltage and the other is the reference voltage. To make these changes a switching signal V_r^{status} is generated locally using the measured voltage from the terminal of the remote wind turbine. The proposed switching logic is presented in Fig. 5. Using the signal V_r^{status}, the

measured voltage input to the PI controller is changed as in Fig. 6. The changes in reference voltage is done according to the logic presented in Fig. 7.
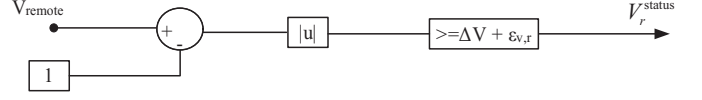

Fig. 5: the status of the voltage at the remote wind turbine terminal
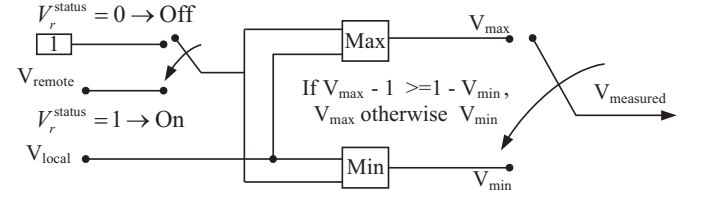

Fig. 6: The modification of the measured voltage input of Figs. 3 and 4 to incorporate the voltage control of a remote wind turbine

If the overvoltage recedes, the voltage controllers on the remote wind turbines are disengaged first before the local wind turbine since the remote wind turbines control the voltage at higher voltage level. This approach minimizes the amount of reactive power used to mitigate an overvoltage as it ensures that the remote wind turbine reactive power is only used when the local reactive power is fully utilized. One should note here that a local RPC is more effective compared to a remote RPC to mitigate an overvoltage.

In general rapid voltage control performances (with response time less than 100 ms) can be obtained by using RPC from wind turbines [32]. But some practical implementation issues related with stability may impose a higher response time (as much as 10 s) [34].

B. Design of the PI controller

To design the PI controller parameters, the bandwidth of the voltage controller can be made sufficiently low so that the dynamics of the inner current and reactive power control loops can be neglected. Fig. 8 shows the equivalent circuit representation of a wind turbine connected to a distribution system. In a steady state, the voltage V_w at the terminal of the wind turbine can be calculated using (7)

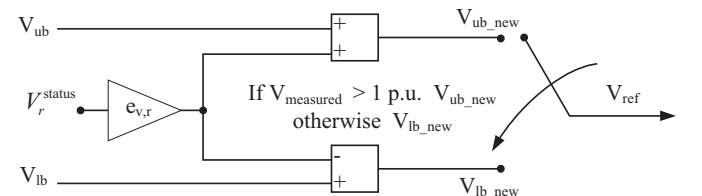$$V_w = E_{th} + \frac{R_{th}P_w + X_{th}Q_w}{V_w} + j\frac{X_{th}P_w - R_{th}Q_w}{V_w} \qquad (7)$$

Fig. 7: Generating the reference voltage

Since $V_w = |V_w| \angle 0^0$, taking the real part gives

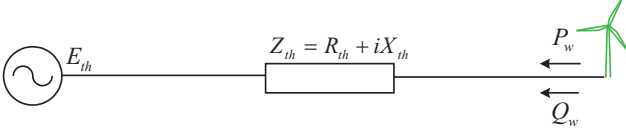$$V_w = E_{th,r} + \frac{R_{th}P_w + X_{th}Q_w}{V_w} \qquad (8)$$

Fig. 8: Equivalent circuit model of a wind turbine connected to a distribution system

Fig. 9 shows the block diagram of the closed loop system where $d = E_{th,r} + \frac{R_{th}P_w}{V_w}$ is considered as a disturbance. If the bandwidth of the closed loop system is chosen to be α_r with

$$\frac{F(s)G(s)}{1+F(s)G(s)} = \frac{\alpha_r}{\alpha_r + s} \qquad (9)$$

and the PI-controller parameters can be set as

$$F(s) = G(s)^{-1}\frac{\alpha_r}{s} \Rightarrow K_I = \frac{\alpha_r V_w^0}{X_{th}} \quad and \quad K_P = 0 \qquad (10)$$
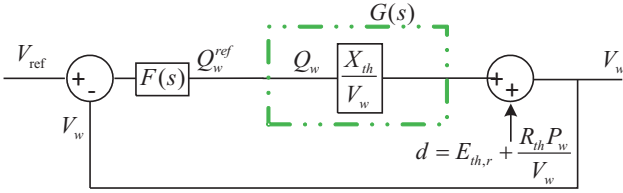

Fig. 9: The block diagram model of the closed loop system

One can use the same PI controller for voltage control at the terminal of a remote wind turbine, as changes in V_w or X_{th} will only change the bandwidth of the voltage control system to a new bandwidth of

$$\alpha_{new} = \frac{\alpha V_w^0 X_{th}^{ac}}{V_w^{ac} X_{th}} \qquad (11)$$

IV. THE COORDINATION OF VOLTAGE REGULATION THROUGH THE SE BASED OLTC CONTROL AND REACTIVE POWER COMPENSATION

When it comes to OLTC based voltage regulation, this paper assumes that the voltage regulation in the distribution system is working satisfactorily before the introduction of wind power. Then, due to the introduction of wind power is the system voltage regulation has become a difficult task. Thus, if the wind turbine regulates the voltage at its terminal, the voltage regulation of the rest of the network can be handled by the OLTC. Moreover, by exempting the OLTC from regulating the highly variable voltage at the terminal of the wind turbine, one is protecting the OLTC from rapid wear and tear that would happen due to frequent tap changes.

The overall voltage regulation structure of the distribution is depicted in Fig. 10. The coordination between the two

controllers can easily be achieved if the voltage measurements from the terminals of the wind turbines are available in the SE process. That is, the OLTC control algorithm knows exactly the voltage level at the wind turbines. Then, due to the inherent time delay present in the OLTC based voltage control, the RPC from the wind turbine mitigates an overvoltage before the OLTC takes any action. On the other hand, if the wind turbine encounters a shortage in reactive power, the overvoltage will persist even after the delay, then the OLTC will take action. To avoid the OLTC from taking action while RPC has regulated the voltage, the deadband of the OLTC needs to be set $> 2 \times (\Delta V + \varepsilon_{v,r})$, e.g. ≈ 0.104 p.u. based on the assumed values above.
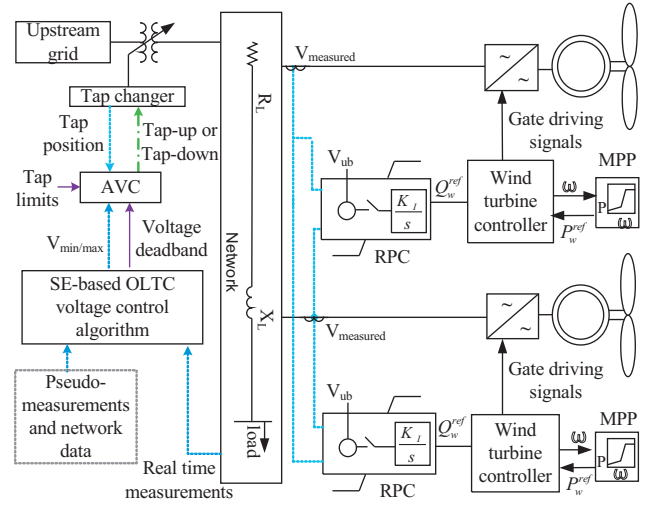

Fig. 10: The general outline of the control and coordination algorithm proposed in this chapter

Without real-time voltage measurement at the wind turbine terminals, the voltage at the wind turbine terminal would be, for example in the case of an overvoltage, overestimated even if the RPC has limited the voltage within the allowed operating deadband. Thus, to coordinate the two voltage controllers even when voltage measurement are not available from the terminals of the wind turbines, the wind turbines should be able to control the voltage at their terminals even at the worst system condition i.e. minimum load and maximum generation. Provided that this holds true, when the SE results show that the voltage at the terminals of the wind turbines is outside the allowed operating range, the SE is rerun with the voltage at the wind turbines' terminals assumed to be at the margin of the allowed operating range. This is because if the RPC is engaged to limit the voltage, it would limit it at the margin of the operating range. Thus, under this coordination approach the role of the OLTC is to control the voltage of only non-wind-turbine buses (i.e. where wind turbine is not installed), and the voltage at the terminals of the wind turbine is assumed to be always kept within the limit by using RPC.

V. CASE STUDY SYSTEM

A. Network and data description

The case study is based on a rural 11kV distribution system operated by Falbygdens Energi located in Falköping area in Sweden. The network is fed by a 40 kV grid through a $45 \pm 8 \times 1.67\%/11.5$ kV, 10 MVA transformer. Our aim is to analyze the applicability of the proposed approach based only one feeder of this distribution system. The circuit diagram of the feeder in consideration is presented in Fig. 11. The feeder consists of 14 buses including the substation busbar (see the Appendix). The voltage in the feeder is to be maintained within $\pm 5\%$ of the nominal value using RPC from the wind turbines and the OLTC of the substation transformer as discussed above. A 50-Hz-sampled load data available from EPFL campus [35] is used to model the load variation in the given distribution system. A one day long 1-Hz-sampled wind power data also available from a 2-MW wind turbine which is scaled and used to model the wind power variation in the system.
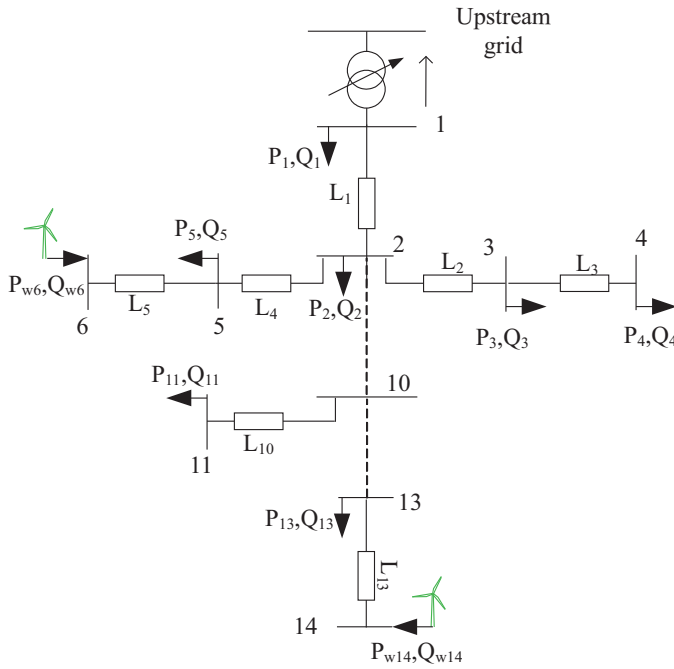

Fig. 11: 14-bus feeder

B. Simulation set up

The software used for simulation is a Matlab/Simulink interface. The electrical network is modeled using the SymPowerSystems toolbox in Matlab. The transformer with the AVC relay and tap changer is modeled using the three-phase OLTC regulating transformer available in SymPowerSystems toolbox. The wind turbine is represented as a simple P-Q load where the available wind power data are used to model the active variation of the wind turbine and the reactive power reference is supplied from the voltage controller. Similarly, the load data obtained from the EPFL campus is used to model the load variation at each bus of the feeder. Moreover, since we are only interested in controlling the rms value of the network

voltage, phasor simulation is used for the analysis. The state estimation is done assuming a balanced three phase system. This is mostly the case in the Nordic distribution system [18]. The refresh rate of the SE depends on the delay time of the tap changer. In our case study, where the delay time of the tap changer is 1 min, the refresh rate is taken to be 1 sec but a lower refresh rate such as 5 sec is found to work well.

C. The results of analysis with the proposed control strategies

1) Voltage regulation using OLTC of the substation transformer: In this section we investigate the results from the proposed SE-based OLTC voltage control. Fig. 12 shows the load (Fig. 12a) and wind power (Fig. 12b) profile of the network. The relatively low magnitude reactive power is omitted from Fig. 12 to keep the presentation simple. Load assigned to Bus 1 includes loads directly connected to the substation as well as those coming from other feeders than the one being investigated. It is assumed that real-time measurement of the voltage magnitude at the substation as well as wind power output and voltage magnitude from Bus 6 are available. However, no measurement is assumed to be available from Bus 14.

As can be inferred from Fig. 12, the load pseudo-measurement data have a constant error of around 35% compared to the actual value while the wind power pseudo-measurement data have a statistical error of around 100% (i.e. for 99.7% of the time the error between the actual and the estimated values is within $\pm 100\%$). The pseudo-measurement data are generated by taking the 10-minute moving average of the actual data and adding a bias to it. The pseudo-measurement data for the load directly connected to the substation bus is not provided in Fig. 12 as this load does not affect the SE process and, hence, is not used in the process.

In practice, load pseudo-measurements can be synthesized based on customer load curves, weather and time of the day data and billing information [36]. Moreover, if there are smart meters in the system, the data available from smart meters would be valuable in setting up more accurate pseudo-measurement data hence better voltage estimate. If no such data are available, the measured power flow at each feeder at the substation bus can be distributed to each bus in proportion to the size of MV/LV substation transformer or recoded maximum power flow at the transformer. The wind power pseudo-measurement data can be constructed from weather forecast data.

With the real-time and pseudo-measurement load and wind power data, the SE algorithm (DSSE block in Fig. 1) provides the voltage estimate at different buses in the network. Figs. 13a and 13b show the actual and the estimated maximum and minimum voltage level in the network. The minimum voltage estimation appears to be more accurate than the maximum voltage. But this is due to the fact that the minimum voltage occurs at the substation where the voltage is measured while the maximum voltage occurs at Bus 14 which is not measured. Fig. 13c shows the input signal fed to the AVC relay by the voltage level analyzer block of Fig. 1. Then the AVC relay initiates a tap changer operation and the resulting tap positions are shown in Fig. 13d.
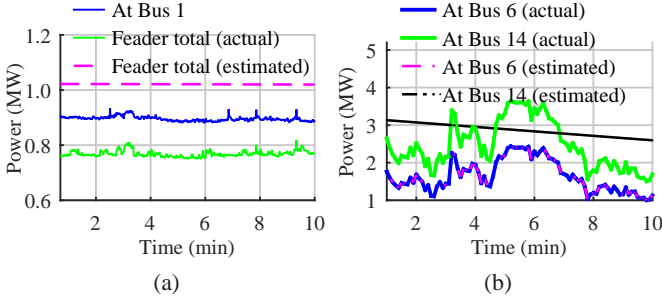
Fig. 12: (a) Load profile and (b) wind power output at different buses in the network
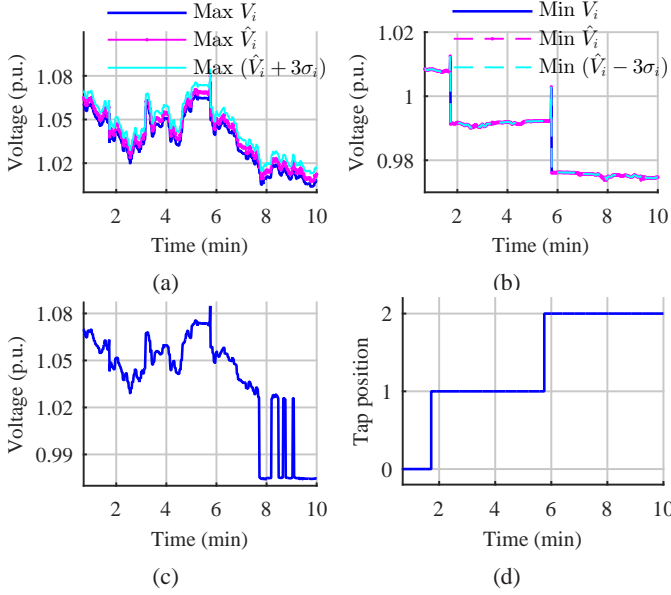

Fig. 13: (a) The actual and estimated maximum b) and minimum voltage of the network, c)the $V_{\min/\max}$ signal fed to the AVC relay by the voltage level analyzer, and (d) the position of the tap changer

From Figs. 13a and 13d one can see that whenever the voltage estimate, i.e. $\text{Max}(\hat{V}_i + 3\sigma_i)$, goes outside the $\pm5\%$ deadband for over one minute (the delay time of the tap changer) the tap changer acts to bring the voltage within the deadband. Overall Figs. 13a and 13d show that the proposed SE-based OLTC voltage control regulates the voltage in the network effectively with limited real-time measurement data from the network. That is, it does not fail to act whenever the voltage is outside the deadband. It can, however, unnecessarily operate the tap changer even when the actual voltage in the network is within the deadband due to the overestimation of the voltages at different buses. For example, in Fig. 13a, the actual voltage is not above 1.05 p.u. for the whole duration between Minute 1 and Minute 2 but the estimated is. This means the tap changer operates unnecessarily at Minute 2. In this case, however, even if voltage measurement is available from Bus 14, the tap change can only be delayed to minute 4 but will not avoided. In general the more measurements are available the less will be the number of unnecessary tap changes.
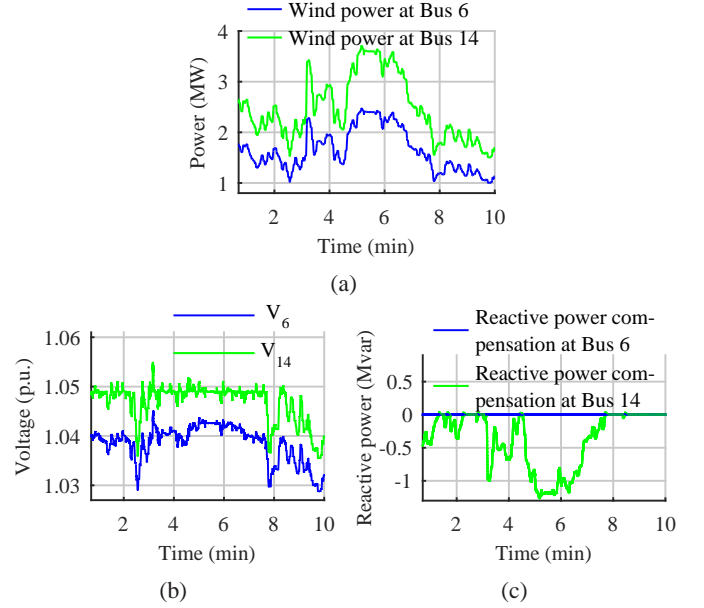

Fig. 14: (a) Wind power profile, b) voltage profile, and c) reactive power profile of the wind turbines at Bus 6 and 14

2) Voltage Regulation using reactive power compensation from the wind turbines: In this section our main focus is to show the results when RPC is utilized to mitigate an overvoltage at the terminal of a local or remote wind turbine. Thus the operation of the tap changer is disabled. The same load and wind power data shown in Fig. 12 are used for the analysis. The wind power outputs of the wind turbines at Bus 6 and 14 are shown again in Fig. 14a for the clarity of the presentation. In Fig. 14b the voltages at the terminals of the wind turbines are shown. Fig. 14c shows the reactive power consumed by the wind turbines.

One can observe from Fig. 14 that with the help of RPC, the voltage at the terminal of the wind turbines is kept within $\pm5\%$ except for short time voltage overshoots. Moreover, Fig. 14c shows that reactive power is consumed only when the voltage is outside the $\pm5\%$ deadband, as desired. The same figure shows also that it is only the wind turbine at Bus 14 that is involved with RPC. This is because the overvoltage occurs only at the terminal of this wind turbine. Note here that without the RPC by the wind turbine, the voltage at Bus 14 could have risen as much as 1.08 p.u. between Minute 5 and 6.

Assume now that wind turbine at Bus 14 has a limited reactive power capability of 1 Mvar while it needs a maximum value of 1.2 Mvar reactive power. As a result, as shown in Fig. 15, the voltage at Bus 14 is outside the $\pm5\%$ deadband between minute 5 and 6 due to the limited reactive power capability of the wind turbine at Bus 14. Nonetheless, with the right communication signals between wind turbines at Bus 6 and 14 this voltage rise can be avoided with the help of RPC from the wind turbine at Bus 6. This is presented in Fig. 16. From Fig. 16 one can see that whenever the wind turbine hits its reactive power limit, the voltage at Bus 14 keeps increasing until it reaches 1.051 p.u. at which point the wind turbine at Bus 6 engages in RPC (see Fig. 16b) to limit the overvoltage
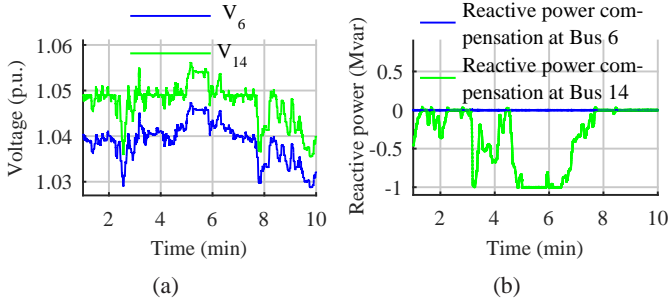
Fig. 15: a) voltage profile, b) reactive power profile of the wind turbines at Bus 6 and 14 when there is a limited reactive power at Bus 6
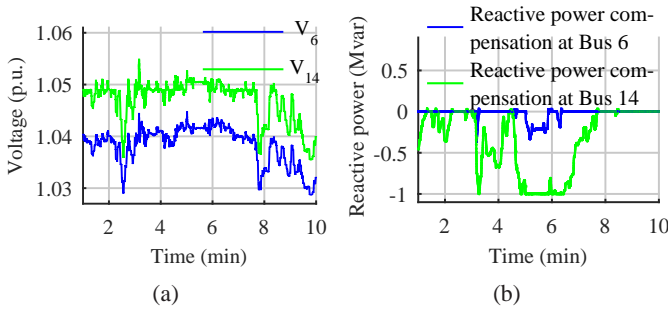

Fig. 16: a) voltage profile, and b) reactive power profile of the wind turbines at Bus 6 and 14 when the RPC is coordinated

Fig. 17: a) The actual and estimated minimum and maximum voltage of the network, b) the reactive power compensation by the wind turbines, and (c) the position of the tap changer

at 1.051 p.u. (see Fig. 16a).

3) Voltage regulation with both OLTC and reactive power compensation: This section combines the two voltage controllers, i.e. the SE-based OLTC and the RPC, and investigates the overall performance of the two control strategies. As mentioned in Subsection V-C1, there is no measurement from wind turbine at Bus 14. So the corresponding method discussed in Section IV is used to coordinate the voltage regulation based on OLTC and RPC. The results of the simulation are shown in Fig. 17. Since the SE adjusts its voltage estimate assuming that the RPC will take care of the voltage at the wind turbine terminal, there is no tap change. If such adjustments were not made, the SE would have overestimated the voltage at Bus 14 and there would have been tap changes similar to the ones in Fig. 13d. Moreover, between Minute 5 and 6 the voltage at Bus 14 is above 1.05, i.e. it is 1.051, due to voltage control coordination principle adopted between the two wind turbines. If real-time measurements from Bus 14 were used in the SE, this would have induced a tap change. To avoid a tap change happening in such cases one may relax the deadband by 0.002p.u. or reduce the value of ΔV in voltage control algorithm of the wind turbines by 0.001.

The presentation so far has used the same load and wind power data to test the effectiveness of the voltage regulation algorithms proposed in this paper. However, though not presented here, the algorithms are tested with different load data and wind power data and are found to successfully carry out the task of voltage regulation in the given radial distribution system. Moreover, in the analysis so far no measurement is assumed to be available from the wind turbine at Bus 14 in
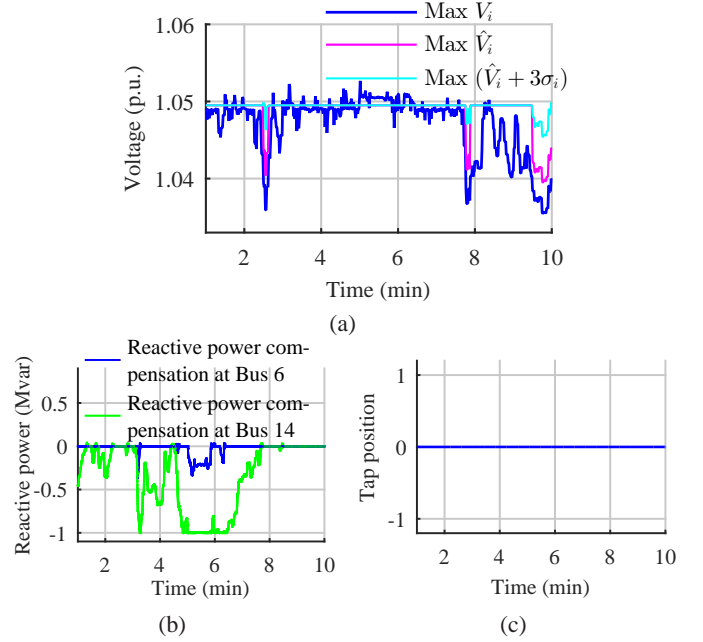
the SE algorithm. This is done to test more clearly the SE algorithm, hence the effectiveness of the OLTC based voltage control algorithm, and the coordination between the RPC and the SE-based OLTC voltage control algorithm. Generally, it is always better to have measurements from the wind turbine buses as

- wind turbine buses are the most likely places where an overvoltage can happen and it is thus better to measure it than to estimate it,
- wind power outputs are less certain and can be of higher magnitude than load buses and with measurement at the wind turbine buses a better voltage estimate of the network would be achieved,
- and finally one can achieve a better coordination between the RPC and the SE-based OLTC voltage control system.

VI. CONCLUSION

This paper has proposed and successfully demonstrated the control and coordination of an SE-based OLTC voltage control and RPC to regulate the voltage level in a given distribution system. The SE-based OLTC voltage control with relaxed deadband shows a good voltage regulating capability and its implementation is much simpler than adjusting the set point of the OLTC. Reactive power from a wind turbine can be used to mitigate an overvoltage that occurs locally as well as at the terminal of any remote wind turbine on the same feeder when the remote wind turbine has a limited reactive power capability to mitigate overvoltage at its terminal. In this way, unnecessary tap regulation is avoided. Unnecessary tap regulation is further avoided when the SE algorithm is adjusted to reflect the effect of reactive power control from the wind turbines in the distribution system.

APPENDIX

TABLE I: network data

From Bus	to Bus	Resistance [Ω]	Reactance [Ω]
1	2	0.34	0.25
2	3	0.66	0.21
3	4	0.97	0.17
2	5	1.93	0.32
5	6	0.22	0.04
2	7	0.27	0.29
7	8	0.23	0.25
8	9	0.23	0.24
9	10	0.24	0.22
10	11	0.17	0.05
10	12	0.15	0.12
12	13	0.65	0.05
13	14	0.43	0.07

REFERENCES

[1] S. N. Liew and G. Strbac, "Maximising penetration of wind generation in existing distribution networks," *Gener. Transm. Distrib. IEE Proceedings-*, vol. 149, no. 3, pp. 256 –262, may 2002.

[2] S. N. Salih, P. Chen, O. Carlson, and N. Shemsedin, "Maximizing Wind Power Integration in Distribution System," in *10th Int. Work. Large-Scale Integr. Wind Power into Power Syst. as well as Transm. Networks Offshore Wind Power Plants*, U. Betancourt and T. Ackermann, Eds., no. 1. Aarhus: Energynautics GmbH, oct 2011, pp. 625–628.

[3] P. Siano, P. Chen, Z. Chen, and A. Piccolo, "Evaluating maximum wind energy exploitation in active distribution networks," *Gener. Transm. Distrib. IET*, vol. 4, no. 5, pp. 598 –608, may 2010.

[4] S. N. Salih, P. Chen, O. Carlson, and L. B. Tjernberg, "Optimizing Wind Power Hosting Capacity of Distribution Systems Using Cost Benefit Analysis," *IEEE Trans. Power Deliv.*, vol. PP, no. 99, pp. 1–1, 2014.

[5] H. Y. Li and H. Leite, "Increasing distributed generation using automatic voltage reference setting technique," in *2008 IEEE Power Energy Soc. Gen. Meet. - Convers. Deliv. Electr. Energy 21st Century*, 2008, pp. 1–7.

[6] P. Esslinger and R. Witzmann, "Regulated distribution transformers in low-voltage networks with a high degree of distributed generation," in *2012 3rd IEEE PES Int. Conf. Exhib. Innov. Smart Grid Technol. (ISGT Eur.*, 2012, pp. 1–7.

[7] M. A. Azzouz, H. E. Farag, and E. F. El-Saadany, "Fuzzy-based control of on-load tap changers under high penetration of distributed generators," in *2013 3rd Int. Conf. Electr. Power Energy Convers. Syst.*, 2013, pp. 1–6.

[8] M. S. El Moursi, H. H. Zeineldin, J. L. Kirtley, and K. Alobeidli, "A Dynamic Master/Slave Reactive Power-Management Scheme for Smart Grids With Distributed Generation," *IEEE Trans. Power Deliv.*, vol. 29, no. 3, pp. 1157–1167, jun 2014.

[9] C. M. Hird, H. Leite, N. Jenkins, and H. Li, "Network voltage controller for distributed generation," *Gener. Transm. Distrib. IEE Proceedings-*, vol. 151, no. 2, pp. 150–156, 2004.

[10] M. Fila, D. Reid, G. Taylor, P. Lang, and M. Irving, "Coordinated voltage control for active network management of distributed generation," in *2009 IEEE Power Energy Soc. Gen. Meet.*, 2009, pp. 1–8.

[11] A. E. Kiprakis and A. R. Wallace, "Maximising energy capture from distributed generators in weak networks," *Gener. Transm. Distrib. IEE Proceedings-*, vol. 151, no. 5, pp. 611 – 618, sep 2004.

[12] P. M. Carvalho, P. F. Correia, and L. Ferreira, "Distributed Reactive Power Generation Control for Voltage Rise Mitigation in Distribution Networks," *IEEE Trans. Power Syst.*, vol. 23, no. 2, pp. 766 –772, may 2008.

[13] E. Demirok, D. Sera, P. Rodriguez, and R. Teodorescu, "Enhanced local grid voltage support method for high penetration of distributed generators," in *IECON 2011 - 37th Annu. Conf. IEEE Ind. Electron. Soc.*, 2011, pp. 2481–2485.

[14] K. Turitsyn, P. Šulc, S. Backhaus, and M. Chertkov, "Options for control of reactive power by distributed photovoltaic generators," in *Proc. IEEE*, vol. 99, no. 6, 2011, pp. 1063–1073.

[15] V. Calderaro, G. Conio, V. Galdi, G. Massa, and A. Piccolo, "Optimal Decentralized Voltage Control for Distribution Systems With Inverter-Based Distributed Generators," *IEEE Trans. Power Syst.*, vol. 29, no. 1, pp. 230–241, 2014.

[16] T. Sansawatt, L. F. Ochoa, and G. P. Harrison, "Smart decentralized control of DG for voltage and thermal constraint management," *IEEE Trans. Power Syst.*, vol. 27, no. 3, pp. 1637–1645, 2012.

[17] I. Leisse, O. Samuelsson, and J. Svensson, "Coordinated voltage control in medium and low voltage distribution networks with wind power and photovoltaics," in *2013 IEEE Grenoble Conf.* IEEE, jun 2013, pp. 1–6.

[18] A. Kulmala, S. Repo, and P. Jarventausta, "Coordinated Voltage Control in Distribution Networks Including Several Distributed Energy Resources," *IEEE Trans. Smart Grid*, vol. 5, no. 4, pp. 2010–2020, jul 2014.

[19] F. Bignucolo, R. Caldon, and V. Prandoni, "Radial MV networks voltage regulation with distribution management system coordinated controller," *Electr. Power Syst. Res.*, vol. 78, no. 4, pp. 634–645, apr 2008.

[20] H. E. Z. Farag and E. F. El-Saadany, "A Novel Cooperative Protocol for Distributed Voltage Control in Active Distribution Systems," *IEEE Trans. Power Syst.*, vol. 28, no. 2, pp. 1645–1656, 2013.

[21] K. M. Muttaqi, A. D. T. Le, M. Negnevitsky, and G. Ledwich, "A Coordinated Voltage Control Approach for Coordination of OLTC, Voltage Regulator, and DG to Regulate Voltage in a Distribution Feeder," *IEEE Trans. Ind. Appl.*, vol. 51, no. 2, pp. 1239–1248, mar 2015.

[22] European Commission, "Cost-benefit analyses & state of play of smart metering deployment in the EU-27," European Commission, Tech. Rep., 2014.

[23] M. Baran and A. Kelley, "A branch-current-based state estimation method for distribution systems," *IEEE Trans. Power Syst.*, vol. 10, pp. 483–491, 1995.

[24] W. M. Lin, J. H. Teng, and S. J. Chen, "A highly efficient algorithm in treating current measurements for the branch-current-based distribution state estimation," *IEEE Trans. Power Deliv.*, vol. 16, pp. 433–439, 2001.

[25] M. Biserica, Y. Besanger, R. Caire, O. Chilard, and P. Deschamps, "Neural Networks to Improve Distribution State Estimation –Volt Var Control Performances," *IEEE Trans. Smart Grid*, vol. 3, no. 3, pp. 1137–1144, 2012.

[26] K. Li, "State estimation for power distribution system and measurement impacts," *IEEE Trans. Power Syst.*, vol. 11, no. 2, pp. 911–916, 1996.

[27] R. Singh, B. C. Pal, and R. A. Jabr, "Choice of estimator for distribution system state estimation," *Gener. Transm. Distrib. IET*, vol. 3, no. 7, pp. 666–678, jul 2009.

[28] T. Ackermann, *Wind Power in Power Systems.* John Wiley & Sons, apr 2005.

[29] O. Anaya-Lara, N. Jenkins, J. Ekanayake, P. Cartwright, and F. M. Hughes, *Wind Energy Generation: Modelling and Control.* John Wiley & Sons, jan 2009.

[30] R. Pena, J. Clare, and G. Asher, "Doubly fed induction generator using back-to-back PWM converters and its application to variable-speed wind-energy generation," *IEE Proc. - Electr. Power Appl.*, vol. 143, no. 3, p. 231, 1996.

[31] H. J.-b. H. Jia-bing, H. Y.-k. H. Yi-kang, and Z. J. G. Z. J. Guo, "The Internal Model Current Control for Wind Turbine Driven Doubly-Fed Induction Generator," *Conf. Rec. 2006 IEEE Ind. Appl. Conf. Forty-First IAS Annu. Meet.*, vol. 1, no. c, pp. 209–215, 2006.

[32] A. D. Hansen and G. Michalke, "Modelling and control of variable-speed multi-pole permanent magnet synchronous generator wind turbine," *Wind Energy*, vol. 11, no. 5, pp. 537–554, sep 2008.

[33] M. Bongiorno, "On Control of Grid-connected Voltage Source Converters," PhD, Chalmers University of Technology, 2007.

[34] K. Clark, N. W. Miller, and J. J. Sanchez-Gasca, "Modeling of GE wind turbine-generators for grid studies," Tech. Rep., 2010.

[35] "EPFL Smart Grid." [Online]. Available: http://smartgrid.epfl.ch/

[36] A. K. Ghosh, D. L. Lubkeman, and R. H. Jones, "Load modeling for distribution circuit state estimation," *Power Deliv. IEEE Trans.*, vol. 12, no. 2, pp. 999–1005, apr 1997.

Shemsedin Nursebo Salih was born on March 10, 1983 in Ethiopia. He studied his B.Sc. in electrical engineering at Arba Minch University, Ethiopia. He did his M.Sc. in power engineering at Chalmers university of Technology, Sweden, from where he graduated in 2010. Now he is doing his PhD degree

at Chalmers University of technology. His research area is wind power integration in distribution system.

Peiyuan Chen (S'2007, M'2010) received his B.Eng. degree in Electrical Engineering from Zhejiang University, China, in 2004, M.Sc. degree in Electric Power Engineering from Chalmers University of Technology, Sweden, in 2006, and PhD degree in Stochastic Modelling and Analysis of Power System with Renewable Generation from Aalborg University, Denmark, in 2010. Currently, he is assistant professor at both Aalborg University and Chalmers University of Technology. His main research interests are optimal operation and planning of power system with integration of wind power.